Bubble Dynamics Investigation in a Slurry Bubble Column

Chengtian Wu, Kelsey Suddard, and Muthanna H. Al-Dahhan
Chemical Reaction Engineering Laboratory (CREL), Dept. of Energy, Environmental and Chemical Engineering (EECE), Washington University in St. Louis, St. Louis, MO 63130

DOI 10.1002/aic.11459
Published online March 11, 2008 in Wiley InterScience (www.interscience.wiley.com).

The application of four-point optical probe has been for the first time extended to a slurry system in a 10.2-cm ID column. Bubble dynamics (local gas holdup, bubble chord length, bubble velocity, bubble frequency, and specific interfacial area) were investigated using an air–water-catalyst system under atmospheric pressure. With an increase in solids loading, the local gas holdup, specific interfacial area, and bubble frequency decreased, while the bubble velocity changed slightly. Bubble chord length increased noticeably, and the bubble chord length distribution spread more widely at high solids loading. It has also been found that the probe orientation is important for an investigation using probes, especially in the wall region of the column. © 2008 American Institute of Chemical Engineers *AIChE J,* 54: 1203–1212, 2008
Keywords: slurry bubble column, four-point optical probe, bubble chord length, bubble velocity

Introduction

With the increasing demand for alternative energy resources and cost effective clean (essentially sulphur and aromatic free) liquid fuel, Fischer-Tropsch (FT) synthesis is attracting more industrial interest. In FT synthesis, synthesis gas (syngas), a mixture of hydrogen and carbon monoxide, obtained from natural gas, or coal, or biomass, is converted to liquid fuels. FT synthesis was discovered in the 1920s, and many kinds of reactors have been employed such as fixed beds, entrained or circulated fluidized beds, and slurry bubble columns. In recent years, however, slurry bubble columns have been found to be the reactor of choice for low temperature (200–280°C) FT synthesis, because they have a much higher capacity than that of the classical fixed bed reactors for low temperature FT synthesis.[1]

Bubble column and slurry bubble column reactors are widely employed in petrochemical, chemical, and biochemical processes, which involve oxidation, hydrogenation, chlorination, alkylation, and polymerization,[2,3] because of their simple installation, easy operation, and high heat and mass transfer rates caused by strong gas–liquid–solid interactions. However, the design, scale-up, and operation of these reactors require detailed knowledge of hydrodynamics, heat and mass transfer, and bubble properties, including bubble size, velocity, frequency, and specific interfacial area.

Techniques including dynamic gas disengagement, video imaging, and microprobes have been developed and utilized to capture bubble dynamic in multiphase reactors. Li and Prakash[4] investigated the influence of slurry concentration on bubble populations and their rise velocities in a 28-cm-diameter slurry bubble column by applying the dynamic gas disengagement technique. They found that the large bubble rise velocity increased with slurry concentration up to 20 vol % and reached an asymptotic value at higher slurry concentrations. Small bubble rise velocity increased with increasing slurry concentration but passed through a maximum at a slurry concentration of about 25 vol %. However, Lee et al.[5] had found that in the coalesced bubble regime, interactions among bubbles are significant, and the dynamic gas disengagement technique is not reliable to measure the bubble size distribution because of the complex bubble characteristics at high superficial gas velocities.

Correspondence concerning this article should be addressed to M. H. Al-Dahhan at muthanna@wustl.edu.

The advantage of the video imaging technique[6–9] is that it does not disturb the flow inside the column during the experiments. However, the video imaging technique requires a transparent wall and liquid, and it is only able to capture the bubble characteristics at low gas holdup conditions in a 2D column and close to the wall in a 3D bubble column. Therefore, its application is limited, because most industrial bubble columns and slurry bubble columns are opaque reactors operating at high superficial gas velocities, pressures, and temperatures.

The microprobe technique, including the conductivity probe (or resistivity probe) and the optical probe, has been frequently used for bubble properties study because of its applicability in opaque systems.[10–15] Conductivity probes utilize the difference in electrical conductivity between the liquid phase and the gas phase. However, the disadvantage of the technique is that it cannot be used with low-conductivity liquids (especially organic liquids which are widely employed in industrial applications) because of the weak signal.

When compared with conductivity probes, optical probes can be employed in both conductive and nonconductive (organic) liquids, and the sensitivity and signal to noise ratio of the optical probe are higher than those of the conductivity probe.[16] Optical probes include single-tip probes, double-tip probes (two-point probes), and multitip probes. Single-tip probes can be used to measure the local gas holdup and bubble frequency. Two-point probes and multi-tip probes are able to capture bubble velocity and bubble chord length in multiphase reactors.[13,14,17] Luo et al.[13] used a two-point probe to measure the bubble size and bubble size distribution in a 10.2-cm-diameter slurry bubble column, and they found that the presence of particles in liquids led to a larger bubble size, especially at ambient pressure. The DOE report[18] found, by applying the same two-point probe in a 5.1-cm-diameter slurry bubble column, that the addition of solids can reduce the bubble rise velocity.

However, based on the error analysis in bubble velocity assuming spherical bubbles, Lim and Agarwal[19] found that the relative error in the bubble velocity measured by two-point probes was susceptible to the incidence angle and the position at which the bubble hits the probe, and the results are theoretically questionable. Xue et al.[17] also analyzed the error in bubble velocity and bubble chord length obtained by two-point probes, with the assumption that the bubble could be spherical or ellipsoidal. Their analysis also indicated that bubble velocity and bubble chord length obtained by two-point probes are subject to large errors. They concluded that two-point probes can be used only in the situations in which all bubbles move strictly in one direction, and are not suitable for systems having complex hydrodynamics, such as the churn turbulent flow regime in bubble and slurry bubble columns.

The four-point optical probe, which was first developed by Frijlink[20] and his colleague, is a promising technique to measure bubble dynamics in bubble columns. In the Chemical Reaction Engineering Laboratory (CREL) at Washington University, a proper algorithm and data processing method for the four-point optical probe signal analysis were developed (Xue et al., unpublished),[15,17] which extends the capability of the probe and improves the accuracy of the measurement. In addition, the specific interfacial area per unit volume can be obtained at the same time. The new algorithm also provides both the magnitude and direction angles of the bubble velocity vector, which means that the probe can be used to measure the velocity of a bubble hitting the probe in various directions. However, the improved technique has been successfully applied only in churn turbulent bubble column flows. There is scarce information and understanding about the bubble dynamics in slurry bubble columns in general and in their churn turbulent flow regime in particular. Accordingly, there is a need to assess and extend the use of the newly developed CREL optical probe in slurry bubble columns.

Therefore, in this study, the application of this improved four-point optical probe was for the first time extended to a slurry system. Local gas holdup, bubble chord length, bubble frequency, interfacial area, and bubble velocity were studied in a 10.2-cm-diameter slurry bubble column, and the effect of superficial gas velocity, solids loading, and radial position on bubble dynamics were investigated.

Experiments

Four-point optical probe (Xue et al., unpublished)[15,17]

The configuration of the modified four-point probe tips is shown in Figure 1. Three peripheral tips form an equilateral triangle, and the fourth tip, which is about 2.0 mm longer than the other three, is positioned in the center of the equilateral triangle. The distance from the central fiber to each of

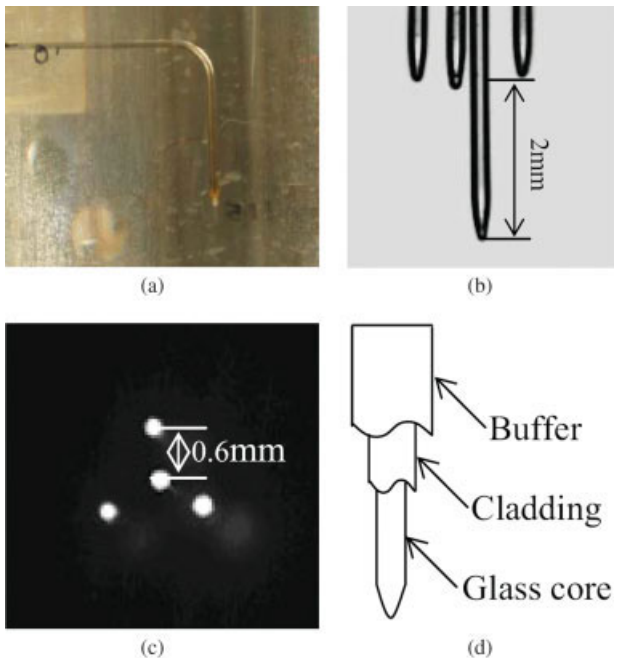

Figure 1. Configuration of the four-point optical probe (not to scale; Xue, 2004).

(a) Picture of the four-point optical probe; (b) side view of the probe tip; (c) bottom view of the probe tip; (d) schematics of the optical fiber. [Color figure can be viewed in the online issue, which is available at www.interscience.wiley.com.]

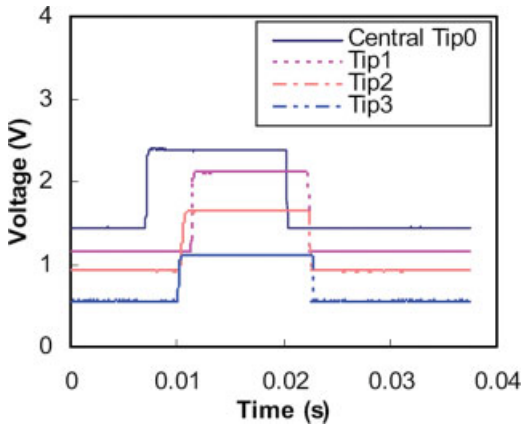

Figure 2. Response of a bubble passing by the four-point optical probe.

[Color figure can be viewed in the online issue, which is available at www.interscience.wiley.com.]

the other three is about 0.6 mm. Hence, the overall diameter of the tip is less than 1.2 mm. Each optical fiber (600 μm in diameter) contains a glass core (200 μm in diameter), a cladding, and a protective layer. As shown in Figure 1c, at the tip of each optical fiber, the cladding and protective layer are removed, and the glass core is formed into a cone shape by a hydrogen flame. Behind the probe tips, all the four optical fibers are glued together and inserted into an L shape stainless steel tube with 1/8 in. outer diameter. To prevent leakage, Epoxy glue surrounds both the tube entry and the bundle fibers.

The optical fiber probe is connected with standard glass fiber connectors to an electronic unit developed by Kramers Laboratory at the University of Delft. A laser beam from a light-emitting diode is sent into each optical fiber, and the reflected light signals from the probe tips are received and transformed into voltage. Finally, the voltage signals are collected by a data acquisition board (PowerDAQ PD2-MFS-8-1M/12) at a sampling frequency of 40 kHz.

The response signal of a bubble vertically hitting the probe in a bubble column is shown in Figure 2. When a single bubble rising vertically hits the four-point optical probe, the central fiber responds first since it is the longest one, and the other three tips respond later. When the fiber is in the liquid phase, the light is transferred into the liquid, establishing a baseline for each trace as shown in Figure 2. When a bubble hits the fiber, the light reflects, and the voltage rise is captured by the electronic unit, shown as a peak in Figure 2.

Experimental setup

The experiments were performed in a 10.2-cm-inner diameter and 105-cm-high plexiglas column, as shown in Figure 3. Compressed air and tap water were used as the gas phase and liquid phase, respectively. FT catalyst carrier (alumina based catalyst skeleton) with an average diameter of 75 μm was used as the solid phase, and the solids loadings in the experiments were selected to be 9 and 25 vol %. Air was introduced into the bottom of the column through a perforated plate gas distributor with 1.09% open area. The superficial gas velocity varied from 1.3 to 13 cm/s which covers both bubbly and churn turbulent flow regimes. During the experiments the dynamic liquid height was maintained at 90 cm by varying the static height at each studied condition, and a four-point optical probe was installed in the fully developed region with a height (from sparger to the tip of the probe) to column diameter ratio (Z/D) equal to 5.5. For most of the experimental conditions, the probe was installed pointing downward. However, for selected experiments, to study the bubble velocity distribution and the effect of probe orientation, the probe was installed pointing both downwards and upwards.

This size of the column was used to assess the applicability of the four-point optical probe in a slurry system at different solids loadings. However, for further investigation of the bubble dynamics of slurry bubble columns using this probe, a larger column diameter is recommended to avoid the wall effect and to examine the effect of reactor scale on the studied parameters.

Results and Discussion

Detailed information about the signal analysis methodology in a bubble column is available in previous studies (Xue et al., Unpublished).[15,17] Local gas holdup, bubble chord length, specific interfacial area, bubble velocity, and bubble frequency can be obtained at the same time. In the slurry system, we found that the addition of fine particles did not disturb the captured signal. Even though the white noise in the base increased, the signal to noise ratio was still good enough for signal analysis. Results and discussion of the measured bubble dynamic parameters in the studied slurry system are as follows.

Local gas holdup

From the response of the probe's tip, the local gas holdup can be obtained as

$$\varepsilon_{g,\mathrm{T}} = \frac{\text{Time spent by the probe's tip in bubbles}}{\text{Total measurement time}} = \frac{T_G}{T},$$

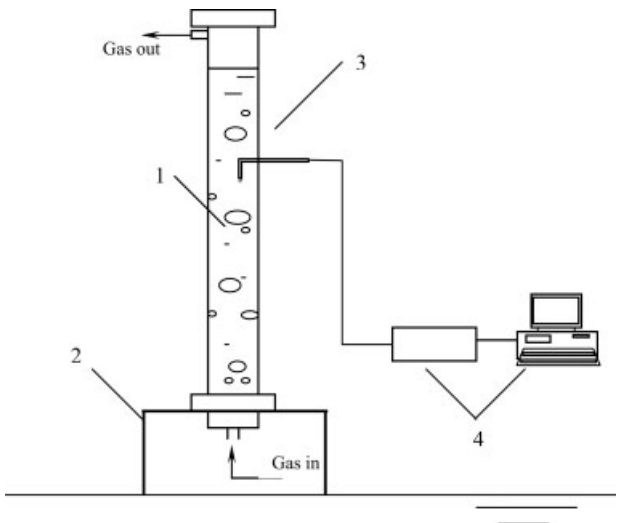

Figure 3. Schematics of the experimental setup.

1, Slurry bubble column (10.2-cm ID, 105 cm high); 2, bottom frame; 3, four-point optical probe; 4, data acquisition system.

where $\varepsilon_{g,T}$ is the time base local gas holdup, T_G is the time the probe tip spends in the gas phase (bubbles), and T is the total measuring time.

Figure 4a shows the time averaged local gas holdup in the center ($r/R = 0.0$, where r is radial position of the probe, and R is the radius of the column) and wall region ($r/R = 0.9$) of the column at different solids loadings. Gas holdup increases with an increase in superficial gas velocity (Ug) at all solids loading both in the center and the wall regions, and the increase of gas holdup becomes smaller at high superficial gas velocities. However, with the increase in solids loading, the gas holdup decreases in both regions. This phenomenon is consistent with other reported results.[5,9,12,21] It is believed that an increase in solids loading increases the apparent viscosity of the pseudo-slurry phase and then enhances the bubble coalescence rate.[3] These effects tend to increase the mean bubble size, and the fast effusion of these large bubbles reduces gas holdup. Radial profiles of gas holdup with superficial gas velocity at 2 and 13 cm/s are shown in Figure 4b. At low superficial gas velocity (2 cm/s) the differences between the gas holdups in the center and in wall region are smaller than those at high superficial gas velocities. Thus, at high superficial gas velocity (13 cm/s) the radial gas holdup profile becomes more parabolic, and the value in the center is much higher than that in the wall region. These phenomena can be explained by the following results of the studies of bubble chord length and bubble frequency.

To compare with previous studies, the cross-sectional gas holdup, $\overline{\varepsilon_g}$, was calculated from the radial profile of the gas holdup, $\varepsilon_g\left(\frac{r}{R}\right)$, as follows: $\overline{\varepsilon_g} = 2\int_0^1 \frac{r}{R}\cdot\varepsilon_g\left(\frac{r}{R}\right)\cdot d\left(\frac{r}{R}\right)$.

This equation is based on the assumption that the holdup profile in a single plane, obtained by averaging the values obtained at equivalent + and − r/R locations, is representative of the azimuthally averaged value. Figure 4c shows the comparison between the estimated cross-sectional gas holdups in this work and the values reported in a 0.10-m ID air–water bubble column under ambient pressure.[1] The results in this work compare well with the reported values at the studied conditions, which further proves the reliability of the four-point probe technique.

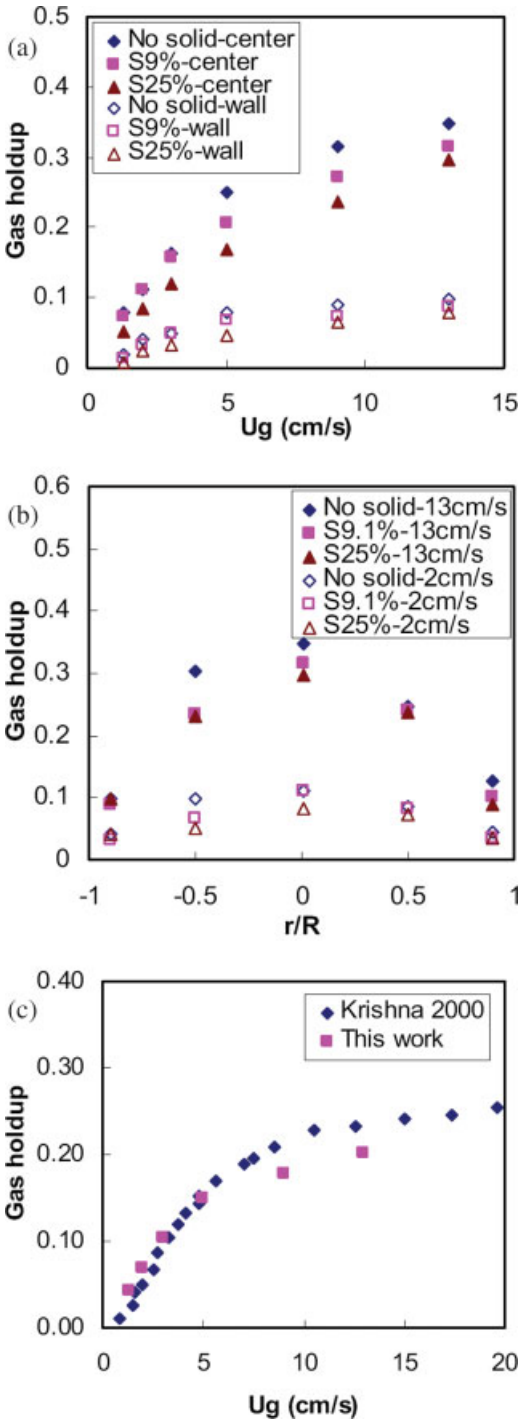

Figure 4. Gas holdup measured by four-point optical probe.

(a) Local gas holdup vs. Ug; (b) radial profile of gas holdup; (c) estimated cross-sectional gas holdup compared with reported values in a 10-cm ID air–water bubble column (Krishna and Sie, 2000). [Color figure can be viewed in the online issue, which is available at www.interscience.wiley.com.]

Bubble chord length distribution

The averaged bubble chord lengths and standard deviations obtained at different solids loading are shown in Figure 5. In both the bubble column and the slurry bubble column, bubble chord lengths in the center and wall regions increase with superficial gas velocity, and the increasing rate becomes smaller with increasing superficial gas velocity.

In the air–water system (no solid), at low superficial gas velocities, the averaged bubble chord lengths in the center and in the wall region are small and close to each other, and the values do not change obviously with the change in superficial gas velocity. The standard deviations at these low gas velocities are small compared with other conditions. This means that the flow is in the bubbly flow regime, and the bubbles are uniformly distributed across the column at about similar size. With a further increase in the superficial gas velocity, the difference between the chord length value in the center and that in the wall region becomes large. Large bubbles form and move in the core of the column with an increase in superficial gas velocity, and small bubbles always appear in the wall region of the column. Hence, the flow

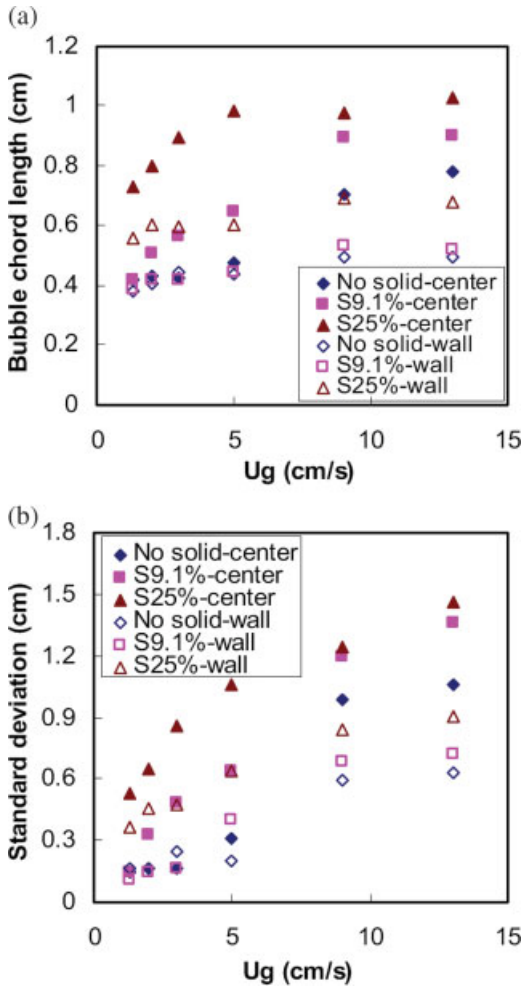

Figure 5. Averaged bubble chord length and standard deviation in a slurry bubble column.

[Color figure can be viewed in the online issue, which is available at www.interscience.wiley.com.]

moves from the bubbly flow regime into the transition flow regime and then the churn turbulent regime.[22] The standard deviation of bubble chord length in the column center at high gas velocities becomes even larger with the increase in gas velocity, and so even in the center of the column, a wide size distribution of bubbles exists at high velocities.

In the slurry system, at low superficial gas velocities the bubble chord lengths in the center region are obviously larger than those in the wall region. The flat stage of the bubble chord length that appears in the air–water system is not found in slurry system. It can also be seen that the bubble chord lengths in the slurry system are larger than those in the air–water system. Especially at 25 vol %, the bubble chord lengths in both the center and wall regions increased noticeably compared with those in the air–water system. Hence, with the addition of fine catalyst particles, large bubbles formed across the column. The standard deviations in the slurry system are also larger than that in the air–water system.

The bubble chord length values at low velocities in the air–water system in this work compared well with those obtained by Saxena et al.[12] and by Bordel et al.[23] The bubble chord lengths in a slurry system (ε_s = 13 vol %) reported by Yasunishi et al.[24] fall in between of the values obtained at solids loading of 9.1 and 25 vol % in this study at similar superficial gas velocities.

The bubble chord length distributions in the column center region at different superficial gas velocities and solids loadings are shown in Figure 6. At each condition, more than 1500 bubbles are considered for the bubble chord length distribution. With an increase in solids loading, the distribution of bubble chord length becomes wider, and the probability of large bubble chord length increases. Especially at high solids loading (25 vol %), the probability of the small bubbles decreases and the number of bubbles larger than 0.75 cm

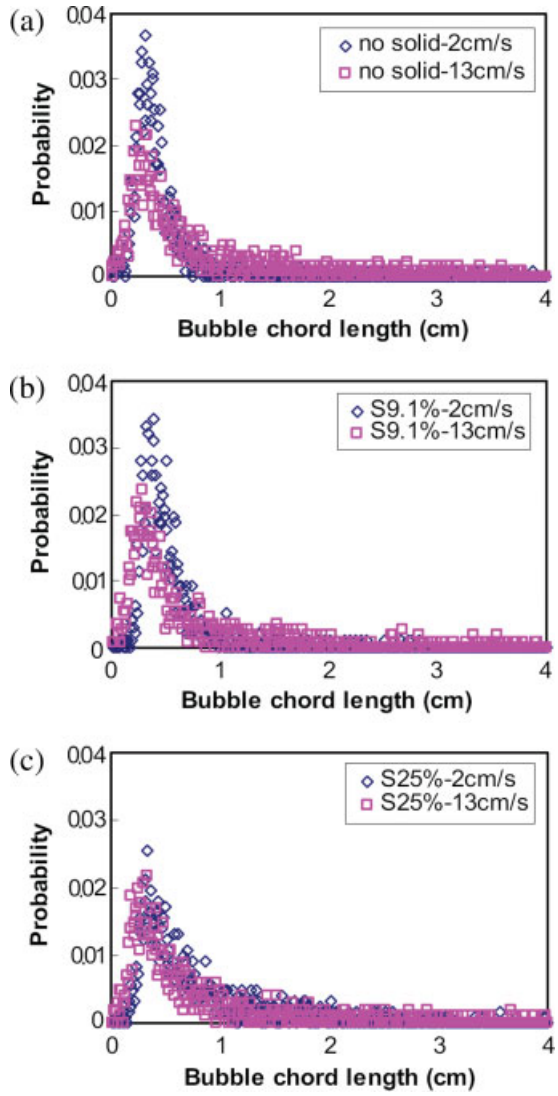

Figure 6. Bubble chord length distribution in the column center at different superficial gas velocity and solids loading.

[Color figure can be viewed in the online issue, which is available at www.interscience.wiley.com.]

increases obviously. Therefore, the addition of fine particles favors the formation of large bubbles, which is consistent with the reported finding by Luo et al.[13]

In the probe measurements, sometimes the apparently small bubble chord lengths measured by the probe may represent large bubbles which are pierced by the probe at their edge. In our experiments, each tip of the four-point optical probe provides a bubble chord length value for a measured bubble. To reduce the mentioned error in measuring the chord length of a large bubble, among the four bubble chord length values provided by the four tips, the largest one was accepted as the measured bubble chord length,[15] which makes the results in this study considerably more close to reality.

Bubble frequency

Dividing the total number of bubbles that hit the probe's central tip by the total sampling time, bubble frequency can also be acquired. As shown in Figure 7, bubble frequency increases with increasing superficial gas velocity but decreases with increasing solids loading. These changes are obvious even in the center of the column. The increasing rate of bubble frequency becomes smaller at high superficial gas velocity. Thus, bubble frequency has a similar trend to local gas holdup, and they are strongly correlated under the experimental conditions studied.

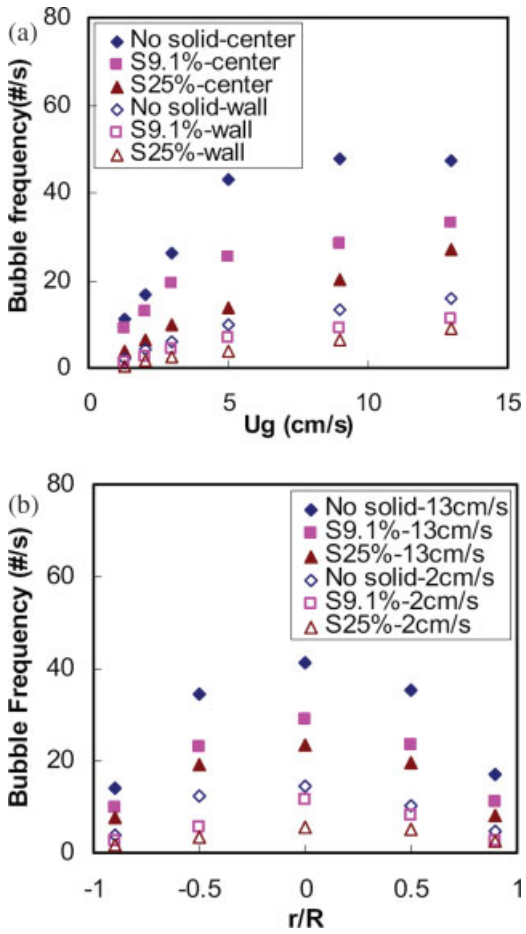

Figure 7. Bubble frequency measured by four-point optical probe.

(a) Bubble frequency vs. Ug; (b) radial profile of bubble frequency. [Color figure can be viewed in the online issue, which is available at www.interscience.wiley.com.]

Combining the findings in the bubble chord length distribution and the bubble frequency, it is not difficult to explain the changes in local gas holdup at different gas velocities and solids loadings. At low velocity, small bubbles uniformly distribute across the column and move at low frequency, which causes low local gas holdup both in the center and wall region of the column. With an increase in superficial gas velocity, bubbles, including the newly formed large bubbles in the center of the column, move at high frequency, which means more bubbles appear in the column, which causes the increase in gas holdup. Most small bubbles still stay in the wall region and move at relatively low frequency. Hence, the gas holdup in the center becomes larger than that in the wall region, and with an further increase in gas velocity, the difference becomes much more obvious.

As mentioned earlier, the addition of fine particles causes the formation of large bubbles, and the average bubble size increases with solids loading under the experimental conditions studied. At the same time, because many small bubbles coalesce to large bubbles, the total number of bubbles decreases, which causes a decrease in the bubble frequency in the slurry system at increasing solids loading. Along with the fast effusion of large bubbles from the column, local gas holdup decreases with increasing solids loading.

Interfacial area

Specific interfacial area is directly related to gas holdup, bubble size, bubble shape, and bubble frequency. Figure 8 shows the effect of superficial gas velocity and solids loading on specific interfacial area and shows the radial profiles with superficial gas velocity at 2 and 13 cm/s. It shows a trend similar to those of the local gas holdup and bubble frequency, both in the center and wall region of the column. Specific interfacial area increases with an increase in superficial gas velocity and decreases with an increase in solids loading. As it is well known, small bubbles have a large surface to volume ratio, and the spherical shape gives minimum surface area. At low velocity, most bubbles are spherical or nearly spherical and move slowly. The increase of gas holdup with superficial gas velocity implies that the number and/or frequency of either small bubbles or large bubbles increase.[25] In addition, as the shape of the large bubbles becomes more irregular at high gas velocity, specific interfacial area increases. However, with the addition of fine particles, more small bubbles combine into larger bubbles, and the bubble frequency also decreases. Hence, the specific interfacial area decreases with increasing solids loading. Sonlikar and Rao[26] measured the specific interfacial area by sodium sulphite oxidation using a cobalt sulphate catalyst in a 10.5-cm-diameter slurry bubble column. They reported a decrease in interfacial area with an increase in particle concentration, which shows the same trend as in this work.

Bubble velocity

The time averaged bubble velocity (probe pointing downward) at different superficial gas velocities and the bubble

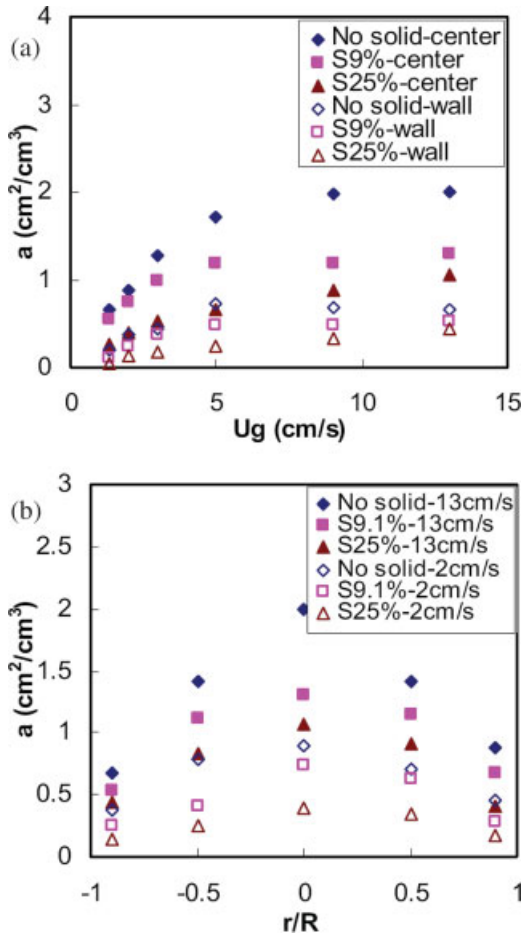

Figure 8. Specific interfacial area measured by four-point optical probe.

(a) Specific interfacial area vs. Ug; (b) radial profile of specific interfacial area. [Color figure can be viewed in the online issue, which is available at www.interscience.wiley.com.]

velocity radial profiles are shown in Figure 9. At all the studied conditions, the standard deviations of the obtained bubble velocity are less than 2.6 cm/s, and they are even lower (less than 1.5 cm/s) at superficial gas velocity. Both in the center and wall region of the column, the rate of increase in bubble velocity is large in the low range of superficial gas velocity but becomes small at high superficial gas velocities. In the center of the column, the changes in bubble velocities at different solids loading are not noticeable under the conditions studied. In the wall region, when the superficial gas velocity is low, the bubble velocity at high solids loading (25 vol %) is larger than those at low solids loadings (9 vol % and no solid). However, at high superficial gas velocity the differences are negligible.

In the bubble velocity distribution analysis, to account for both the upward and downward moving bubbles, the four-point optical probe was installed pointing both downward and upward. We considered bubbles traveling upward to have positive velocities, and those moving downward to have negative velocities. Figure 10 shows the bubble velocity distributions, including all measured upward and downward bubble movements, both in the center and wall region of the column. In the center of the column most bubbles move upward, and the bubble velocity distributions at a given superficial gas velocity are similar at all studied solids loadings. With an increase in superficial gas velocity, the bubble velocity distribution spreads wide, and the number of bubbles moving downwards in the center increases slowly. The above result is consistent with the findings in air–water bubble columns.[15]

In the wall region, at low superficial gas velocity (2 cm/s) the bubble velocity distribution is narrow and sharp compared with that in the center, and only a few bubbles move downwards. With increasing superficial gas velocity the bubble velocity distribution becomes broader, and the ratio of downward moving bubbles increases greatly. Also, the number of bubbles with high velocities increases, which implies the enhancement of the circulation of slurry in the column. At high superficial gas velocity (13 cm/s), the number of bubbles moving downward is equal to or even larger than that moving upward in two-phase systems and in three-phase systems at low solids loading (9 vol %). However, at high

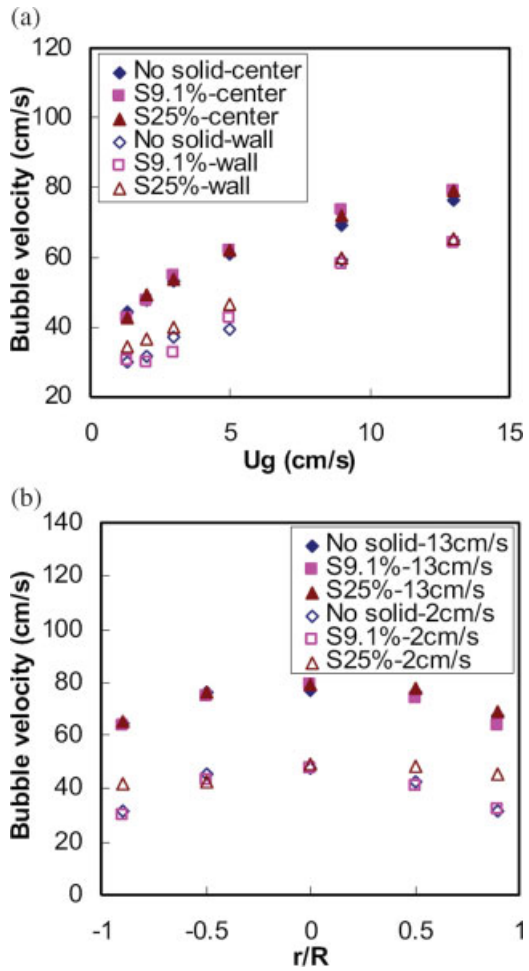

Figure 9. Bubble velocity and its radial profile (probe pointing downward).

(a) Bubble velocity vs. Ug; (b) radial profile of bubble velocity. [Color figure can be viewed in the online issue, which is available at www.interscience.wiley.com.]

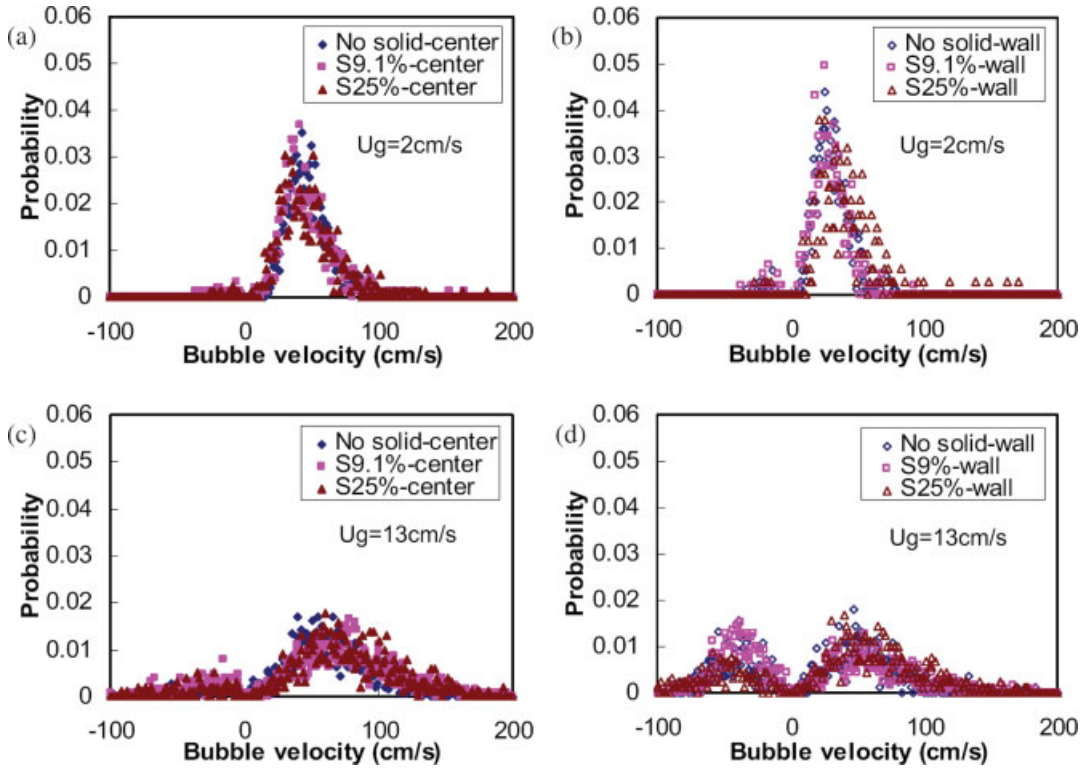

Figure 10. Bubble velocity distribution at different Ug and solids loading.

[Color figure can be viewed in the online issue, which is available at www.interscience.wiley.com.]

solids loading (25 vol %), the number of bubbles moving downward in the wall region is still smaller than that moving upward at the studied conditions.

Effect of probe orientation

To understand the effect of the probe orientation (downward or upward), in the air–water system at selected conditions, the values of the investigated parameters (local gas holdup, bubble chord length, specific interfacial area, and bubble velocity) obtained at both probe directions and both in center and wall regions are listed in Tables 1 and 2. The bubble numbers obtained as part of the signal process are considered as weighting factors to calculate the local average values of each of these parameters. To calculate the average local gas holdup, the number of bubbles that hit the center tip is used, and for the calculations of the average values of the other parameters, the number of bubbles that hit all four tips is applied. The equation used to calculate the averages is as follows.

$$m_{\text{ave}} = \overline{m_{\text{d}}} \cdot f_{\text{d}} + \overline{m_{\text{u}}} \cdot f_{\text{u}}$$

$$\overline{m_{\text{d}}} = \frac{\sum_{i=1}^{N_{\text{d}}} m_{\text{d}i}}{N_{\text{d}}}, \quad \overline{m_{\text{u}}} = \frac{\sum_{j=1}^{N_{\text{u}}} m_{\text{u}j}}{N_{\text{u}}}$$

$$f_{\text{d}} = \frac{N_{\text{d}}}{N_{\text{d}} + N_{\text{u}}}, \quad f_{\text{u}} = \frac{N_{\text{u}}}{N_{\text{d}} + N_{\text{u}}}$$

where m_{ave} is the average of the investigated parameter, $\overline{m_{\text{d}}}$ is the average value of the parameter with probe pointing downward, $\overline{m_{\text{u}}}$ is the average value of the parameter with the probe pointing upward, f_{d} is the weighting factor of the pa-

Table 1. Investigated Parameters at Different Probe Orientations (Ug = 2 cm/s)

	Center (r/R = 0.0)			Wall (r/R = 0.9)		
Investigated Parameter	Probe Pointing Downward	Probe Pointing Upward	Average	Probe Pointing Downward	Probe Pointing Upward	Average
ε (%)	11.2	5.08	8.98	3.96	3.22	3.70
l_{chord} (cm)	0.431	0.093	0.429	0.407	0.394	0.406
a (cm^2/cm^3)	0.889	2.52	0.896	0.370	0.475	0.372
u_{b} (cm/s)	47.9	12.5	47.7	31.3	18.6	31.0

ε, local gas holdup; l_{chord}, bubble chord length; a, specific interfacial area; u_{b}, bubble velocity.

Table 2. Investigated Parameters at Different Probe Orientations (Ug = 13 cm/s)

	Center (r/R = 0.0)			Wall (r/R = 0.9)		
Investigated Parameter	Probe Pointing Downward	Probe Pointing Upward	Average	Probe Pointing Downward	Probe Pointing Upward	Average
ε (%)	34.7	26.9	31.6	9.79	13.1	11.3
l_{chord} (cm)	0.782	0.483	0.766	0.495	0.362	0.444
a (cm^2/cm^3)	2.01	3.78	2.10	0.668	0.555	0.625
u_b (cm/s)	76.1	38.2	74.1	64.7	45.1	57.2

ε, local gas holdup; l_{chord}, bubble chord length; a, specific interfacial area; u_b, bubble velocity.

rameter with the probe pointing downward, f_u is the weighting factor of the parameter with the probe pointing upward, i and j are index number, N_d is the bubble number obtained with the probe pointing downward, and N_u is the bubble number obtained with the probe pointing upward.

In the center region of the column, at both superficial gas velocities (2 and 13 cm/s) the averaged values are much closer to those with the probe pointing downward. This is because the number of downward moving bubbles is still small compared with the number of bubbles traveling upward in the center, and hence the contribution of these downward moving bubbles to the average value is small, even negligible. Therefore, the measured results with the probe pointing downward in the center can represent the local average values.

In the wall region, at the low superficial gas velocity (2 cm/s) the system is still in the bubbly flow regime, and thus the average values are still close to those with the probe pointing downward. However, in the churn turbulent flow regime (Ug = 13 cm/s) the system is much more complex than in the bubbly flow regime. Values acquired with the probe pointing downward and upward are both important to consider calculating the local averaged values. For the other radial positions, especially those close to the wall, the measurement with the probe pointing upward also cannot be neglected.

Remarks

The application of the four-point optical probe developed by Xue[15] was extended to a 10.2-cm-diameter slurry bubble column to study the local gas holdup, bubble chord length, bubble frequency, specific interfacial area, and bubble velocity. With an increase in superficial gas velocity, the local gas holdup, bubble chord length, bubble frequency, specific interfacial area, and bubble velocity increased in both the center and wall regions of the column. Local gas holdup, specific interfacial area, and bubble frequency decreased with an increase in solids loading. With an increase in solids loading, average bubble chord length increased, while bubble velocity changed slightly. Based on bubble chord length distribution in the column center, we found that bubble chord length spread more widely with increasing solids loading. Bubble velocity distribution was analyzed in the center and wall regions of the column. The ratio of bubbles moving downward in the center and wall region increased with increasing superficial gas velocity, and the phenomenon was even apparent in the wall region at low solids loadings. Measurements with the probe pointing both upward and downward are necessary for the bubble dynamic study using probes, especially in the wall region at high superficial velocities.

This work provides important information about bubble dynamics in a slurry system. However, this study was conducted in a small diameter column, in which the wall effect may be still important on the studied parameters, especially at high solids loading. Therefore, for a better understanding of the bubble dynamics in a commercial FT slurry bubble column, further experimentation in larger columns is recommended.

Acknowledgments

The authors thank Professor M. P. Dudukovic for his comments. The financial supports from ConocoPhillips, Eni, GTL-F1 (Statoil), Sasol, and Johnson Matthey are gratefully acknowledged.

Literature Cited

1. Krishna R, Sie ST. Selection, design and scale-up aspects of Fischer-Tropsch reactors. *Fuel Process Technol.* 2000;64:73–105.
2. Deckwer W-D, Alper E. Katalytische suspensions reaktoren. *Chemie Ingenieur Technik.* 1980;52:219–228.
3. Fan L-S. *Gas-Liquid-Solid Fluidization Engineering*. Boston, MA: Butterworth Series in Chemical Engineering, 1989.
4. Li H, Prakash A. Influence of slurry concentrations on bubble population and their rise velocities in a three-phase slurry bubble column. *Powder Technol.* 2000;113:158–167.
5. Lee DJ, Luo X, Fan L-S. Gas disengagement technique in a slurry bubble column operated in the coalesced bubble regime. *Chem Eng Sci.* 1999;54:2227–2236.
6. Idogawa K. Methods for measurement of gas holdup and gas bubble diameter in a high-pressure bubble column. *Kagaku Kogaku.* 1997; 61:781–782.
7. Mihai M, Pincovschi I. Experimental study of bubble size distribution in a bubble column. *Sci Total Environ.* 1998;5:34–41.
8. Marques JJP, Bouard R. Bubbles in a gas-solid fluidized bed photographic characterization. *Tech Modern.* 1999;91:20–24.
9. Vandu CO, Koop K, Krishna R. Large bubble sizes and rise velocities in a bubble column slurry rector. *Chem Eng Technol.* 2004;27: 1195–1199.
10. Burgess JM, Calderbank PH. The measurement of bubble parameters in two-phase dispersions. I. The development of an improved probe technique. *Chem Eng Sci.* 1975;30:743–750.
11. Matsuura A, Fan L-S. Distribution of bubble properties in a gas-liquid-solid fluidized bed. *AIChE J*. 1984;30: 894–903.
12. Saxena AC, Rao NS, Saxena SC. Bubble size distribution in bubble columns. *Can J Chem Eng.* 1990;68:159–161.
13. Luo X, Lee DJ, Lau R, Yang G, Fan L-S. Maximum stable bubble size and gas holdup in high-pressure slurry bubble column. *AIChE J*. 1999;45: 665–680.
14. Mudde RF, Saito T. Hydrodynamical similarities between bubble column and bubbly pipe flow. *J Fluid Mech.* 2001;437:203–228.
15. Xue J. Bubble velocity, size and interfacial area measurements in bubble columns. Ph.D. Thesis, Washington University in St. Louis, St. Louis, MO, 2004.

16. Van der Lans RGJM. PhD Dissertation, Delft University of Technology, Delft, The Netherlands, 1985.
17. Xue J, Al-Dahhan M, Dudukovic MP, Mudde RF. Bubble dynamics measurements using four-point optical probe. *Can J Chem Eng*. 2003;81:1–7.
18. Al-Dahhan M, Fan L-S, Dudukovic MP, Toseland B. Advanced diagnostic techniques for three-phase slurry bubble column reactors (SBCR). Washington University in St. Louis, St. Louis, MO. DOE report DE-FG-26-99FT40594. 2003.
19. Lim KS, Agarwal PK. Bubble velocity in fluidized beds: the effect of non-vertical bubble rise on its measurement using submersible probes and its relationship with bubble size. *Powder Technol*. 1992; 69:239–248.
20. Frijlink JJ. Physical aspects of gassed suspension reactors. Ph.D. Thesis, Delft University of Technology, Delft, The Netherlands, 1987.
21. Kara S, Kelkar BG, Shah YT. Hydrodynamics and axial mixing in a three-phase bubble column. *Ind Eng Chem Process Des Dev*. 1982; 21:584–594.
22. Chen RC, Reese J, Fan L-S. Flow structure in a three-dimensional bubble column and three-phase fluidized bed. *AIChE J*. 1994;40: 1093–1104.
23. Bordel S, Mato R, Villaverde S. Modeling of the evolution with length of bubble size distributions in bubble columns. *Chem Eng Sci*. 2006;61:3663–3673.
24. Yasunishi A, Fukuma M, Muroyama K. Measurement of behavior of gas bubbles and gas holdup in a slurry bubble column by a dual electroresistivity probe method. *J Chem Eng Jpn*. 1986;19:444–449.
25. Krishna R, Wilkinson PM, van Dierendonck LL. A model for gas holdup in bubble columns incorporating the influence of gas density on flow regime transitions. *Chem Eng Sci*. 1991;46:2491–2496.
26. Sonolikar RL, Rao R, TBML. Effective interfacial area in a magnetically stabilized slurry bubble column. *Chem Eng Sci*. 1996;51:2701–2707.

Manuscript received Feb. 9, 2007, revision received Sept. 12, 2007, and final revision received Jan. 20, 2008.